Proceedings of the ASME 2024 43nd International Conference on Ocean, Offshore, and Arctic Engineering
OMAE2024
June 9-14, 2024, Singapore EXPO, Singapore

OMAE2024-121877

RECENT ADVANCES IN THE STUDY OF HYDROGEN EMBRITTLEMENT IN FERRITIC STEELS

Virat Dixit
University of Texas at Arlington
Houston, TX

Anju Mishra
Indian Institute of Technology, Kanpur
Kanpur, India

ABSTRACT

Within sustainable alternatives, hydrogen is regarded as a prospective future fuel by the scientific community. Hence, safe and economically efficient hydrogen storage and transportation methods are required [1]. The interaction of hydrogen with structural materials is one of the major obstacles in developing these storage and transportation techniques. In most cases, interstitial atoms determine the mechanical properties of structural materials. Hydrogen is a common interstitial element, which generally degrades the fracture behavior and leads to premature or catastrophic failure in various materials, known as hydrogen embrittlement [2]. This implies that hydrogen embrittlement can occur in most structural materials, including ferritic steels, an important class of materials [3].

The process behind the hydrogen embrittlement of ferritic steels remains largely unclear despite significant research efforts to understand these mechanisms and create potential mitigating measures [4]. New developments in multi-scale modeling and experimental instruments are beginning to shed light on the embrittlement process of ferritic steels [5]. This report represents a subset of the most recent advancements, highlighting how novel techniques have enhanced our comprehension of the relationships between structure, properties, and performance of ferritic steels under mechanical loading in a hydrogen environment. Next, a thorough analysis of the different embrittlement mechanisms will be presented to investigate the performance of steels in hydrogen. Furthermore, an insight into contemporary methodologies and novel mitigation strategies employed in designing hydrogen embrittlement-resistant steels will be presented.

NOMENCLATURE

E_B	binding energy
n	average number of sites per unit area
H_2	coverage ratio
H	chemisorbed Hydrogen and Hydrogen Concentration
k_{aP}	rate at which molecular H_2 transitions from the gas phase to an adsorbed state
k_d	rate constant for the desorption of H_2 back into the gas phase
K_1	rate constant for the dissociation of adsorbed H_2 into atomic hydrogen
K_2	rate at which atomic, chemisorbed hydrogen recombines into molecular, physisorbed H_2.
k_a	striking Probability
FCGR	fatigue crack growth rate
X70	a kind of steel
J	Hydrogen Flux
D	diffusivity of Hydrogen
Φ	hydrogen permeability
P	pressure of hydrogen in the adjacent gaseous milieu
$[H]_\sigma$	stress-assisted hydrogen concentration hydrostatic stress
R	universal gas constant
V	partial molar volume of hydrogen
Θ	degree of surface coverage
UTS	ultimate tensile strength
v	vibrational Frequency
K_{TH}	threshold stress intensity factor
APT	atom probe tomography
SIMS	secondary ion mass spectrometry
i	i^{th} axis (x,y,z)
M	reduced mass
h	Planck constant
K_B	Boltzmann constant

TDS	thermal desorption spectroscopy

1. INTRODUCTION

This scholarly paper provides a detailed analysis of the ongoing transition in the global energy sector from traditional fossil fuels to more environmentally sustainable sources. Emphasizing the significant role of renewable energy, the paper highlights the advancements in solar cell efficiency and wind power capacity, reflecting a global shift towards eco-friendly energy solutions driven by policy reforms and technological innovations.

Central to this transition is the role of hydrogen as a key energy storage medium, addressing the challenge of aligning the intermittent production of renewable energy with fluctuating energy demands. The paper explores hydrogen's potential in storing excess energy for later conversion to electricity or synthetic natural gas, underscoring its critical importance in the development of clean energy infrastructure. This necessitates the creation of safe, efficient, and economically viable hydrogen storage and transportation methods.

A significant focus of the paper is on the interaction between hydrogen and structural materials, specifically hydrogen embrittlement in metals. It provides a historical perspective on the issue, analyzing how factors like testing conditions and hydrogen-material interactions influence embrittlement in ferritic steels. The paper delves into the debates and research on the mechanisms behind hydrogen embrittlement, highlighting recent advancements in experimental techniques and imaging that have enhanced understanding and informed standards for hydrogen storage and transportation.

Concluding, the paper emphasizes the need for a comprehensive understanding of the structure, properties, and performance of materials exposed to hydrogen, especially ferritic steels. It addresses the detrimental effects of hydrogen on mechanical properties at room temperature, notably ductility, which is crucial for advancing strategies for the safe and efficient use of hydrogen in the clean-energy economy. This review offers both academic and practical insights, contributing to the development of sustainable energy solutions in an environmentally conscious world.

2. BEHAVIORAL DYNAMICS OF HYDROGEN IN METALLIC STRUCTURES

The vulnerability of ferritic steels to hydrogen-induced effects is influenced by a complex interplay of factors, encompassing the steel's microstructural characteristics, the mode of hydrogen integration (whether through electrochemical or gaseous charging), ambient temperature, and the dynamics of deformation, such as strain rates or fatigue frequency. These elements are pivotal in determining the fundamental parameters that dictate hydrogen susceptibility, specifically the concentration of hydrogen within the steel and the kinetics of hydrogen interaction. This assertion is substantiated by the efficacy of embrittlement models that incorporate variables such as hydrogen's interaction with the steel surface, the kinetics of hydrogen ingress into the steel, and its subsequent transport within the steel matrix, including interactions within the crystal lattice, near dislocations, grain boundaries, and vacancies.

In this section, the paper provides an extensive review of both experimental and computational studies focusing on these critical parameters. While there is yet to be a consensus within the scientific community regarding the precise physical mechanisms underlying hydrogen embrittlement in ferritic steel, there is a general agreement about the process by which hydrogen is assimilated into the material. Initially, diatomic hydrogen adsorbs onto the metal surface, subsequently dissociating into atomic hydrogen, which then chemisorbs at the surface. Following this, the hydrogen atoms diffuse through the metal lattice or along grain boundaries, congregating near areas of internal stress, such as dislocations or crack tips. However, the specific behaviors and impacts of hydrogen at this juncture remain a subject of ongoing debate and investigation within the field.

2.1. HYDROGEN ADSORPTION DYNAMICS ON FERRITIC STEEL SURFACES

In the preliminary phase of interaction, molecular hydrogen from the gaseous environment initially adheres to the steel surface in its diatomic form. During the process of gas charging, the transition from gaseous phase hydrogen to its incorporation within the steel involves specific reactions

$$H_2(g) \leftrightarrow H_2(\text{ads.}), \tag{1}$$

$$H_2(\text{ads.}) \leftrightarrow 2H(\text{chem.}). \tag{2}$$

Ransom and Ficalora demonstrated that the adsorption of H_2 on pure iron (Fe) at 77K adheres to the principles of a Langmuir isotherm, indicative of localized adsorption. This process is characterized by a binding energy (Eb) of approximately 60 kJ/mol and a vibration frequency of approximately 24 GHz [6]. Within the framework of the Langmuir model, the degree of surface coverage by adsorbed molecules, denoted by 'θ', is determined by

$$\theta = \frac{P_{\text{vapor}}\chi}{1 + P_{\text{vapor}}\chi}, \tag{3}$$

where Pvapor represents the pressure of the gas. The Langmuir constant, denoted as 'v', corresponding to a specific temperature 'T', is defined by the following expression

$$\chi = \frac{e^{\frac{E_b}{k_B T}}}{\prod_{i=1}^{3} \sinh\left(\frac{h\,\nu_i}{k_B T}\right)} \sqrt{\frac{h^6}{(8\pi M)^3 (k_B T)^5}}, , \tag{4}$$

In this context, 'Eb' represents the binding energy, while 'ν, i' refers to the vibrational frequency along the ith axis (where i equals x, y, z). 'M' stands for the reduced mass, 'h' is the Planck constant, and 'kB' denotes the Boltzmann constant. At standard room temperature, hydrogen achieves near-complete surface coverage (ratio of 1:1 H/Fe) at pressures exceedingly approximately 0.05 MPa.

Advanced ab initio calculations regarding hydrogen desorption temperatures and energies on the (100), (110), (111), and (211) [7] surfaces of iron have yielded an average hydrogen binding energy on Fe of about 274.5 kJ/mol. Notably, the highest binding energy observed is 282.4 kJ/mol on the (110) surface, while the lowest is 266.9 kJ/mol on the (111) surface.

In scenarios involving cathodic charging, where hydrogen is present in an aqueous solution in cationic form, the reaction is characterized as follows:

$$H^+(aq) + e^- \leftrightarrow \left(\frac{1}{2}\right)H_2(g) \leftrightarrow H(chem.). \quad (5)$$

Although the mechanisms through which hydrogen is incorporated into steel differ between gas charging and cathodic charging, both processes can culminate in comparable outcomes in terms of hydrogen embrittlement in steel structures. There have been scholarly endeavors to draw parallels between the conditions of electrochemical charging and an equivalent effective gas-charging pressure (or fugacity). In this context, Atrens and colleagues employed thermal desorption spectroscopy (TDS) to quantitatively assess the hydrogen concentration of both the charging potential and the gas pressure. This analysis was conducted on two types of steel: 980DP and 3.5NiCrMoV. The findings revealed a correlation where the hydrogen concentration escalated in response to an increase in both the negative charging potential and the ambient hydrogen gas pressure.

2.2. DYNAMICS OF ADSORPTION AND CHEMISORPTION PROCESSES

The process of H_2 sorption is a sequential two-stage phenomenon, wherein molecular H_2 initially adheres to the surface, followed by its dissociation into atomic hydrogen. The comprehensive chemisorption rate of H_2 on thin iron films has been quantitatively determined by observing chemisorption-induced alterations in electrical resistivity, as elaborated in [8]. This process has been mathematically modeled utilizing a set of coupled differential equations:

$$\frac{d\Theta^*}{dt} = k_a p(1-\Theta^*) - k_d\Theta^* - \frac{1}{2}\frac{d\Theta}{dt} \quad (6)$$

And,

$$\frac{1}{2}\frac{d\Theta}{dt} = k_1(1-\Theta)^2 - k_2\Theta^2(1-\Theta^*), \quad (7)$$

In this model, 'H_2' denotes the coverage ratio, representing the number of molecular H_2 species per adsorption site, while 'H' signifies the coverage of chemisorbed hydrogen. 'k_ap' is defined as the rate at which molecular H_2 transitions from the gas phase to an adsorbed state. 'k_d' represents the rate constant for the desorption of H_2 back into the gas phase. 'k_1' is the rate constant for the dissociation of adsorbed H_2 into atomic hydrogen, and 'k_2' delineates the rate at which atomic, chemisorbed hydrogen recombines into molecular, physisorbed H_2. The parameter 'k_a' is determined as follows

$$k_a = \frac{\alpha}{\overline{n}\sqrt{2\pi M k_B T}}, \quad (8)$$

In this context, 'a' represents the "sticking probability," while 'n' denotes the average number of sites per unit area. Figure 1(a) illustrates the variation in adsorbed coverage over time for iron (Fe) exposed to hydrogen gas at pressures of 1.7 and 5.5 MPa, demonstrating that full adsorbed hydrogen coverage is achieved within tens of nanoseconds. Conversely, Figure 1(b) depicts the chemisorbed coverage over time, which, as inferred from the coupled differential equations, is largely independent of pressure, except at extremely low gas pressures (<1 Pa). Achieving full coverage through chemisorption requires tens of seconds, thereby making it the rate-limiting step in the accumulation of surface hydrogen for integration into steel. Figure 1 also compares the adsorption and chemisorption rates for deuterium, a hydrogen isotope. Deuterium is chemically identical to hydrogen but differs in having a neutron in its nucleus, effectively doubling its mass. This increased mass significantly slows down the diffusion, chemisorption, and adsorption rates. Comparative studies between hydrogen and deuterium reveal minimal impact on embrittlement in tensile tests, yet a significant influence on fatigue properties dependent on gas pressure. For instance, at a pressure of 1.7 MPa, deuterium does not increase the fatigue crack growth rate (FCGR) of X70 steel, but at 5.5 MPa [9], it does.

These analyses assume the interaction of pure H_2 gas with a pristine Fe surface. However, surface contaminants, such as oxides, significantly affect both the adsorption and dissociation of hydrogen on steel. Ab initio calculations indicate that oxygen, which is preferentially adsorbed onto Fe surfaces, impedes hydrogen adsorption and dissociation. This obstruction of hydrogen dissociation and subsequent diffusion into steel is likely why impurity levels of oxygen in H_2 gas are observed to reduce susceptibility to hydrogen embrittlement and hydrogen-affected fatigue crack growth rate. Predictions suggest a similar influence on hydrogen dissociation kinetics by carbon monoxide, which also reduces hydrogen susceptibility. However, these calculations do not indicate strong prevention of hydrogen dissociation due to CH_4 or CO_2, and correspondingly, hydrogen susceptibility is not significantly affected by these gases. Therefore, the kinetics of hydrogen adsorption, dissociation, and chemisorption appear to play a pivotal role in the phenomenon of hydrogen embrittlement.

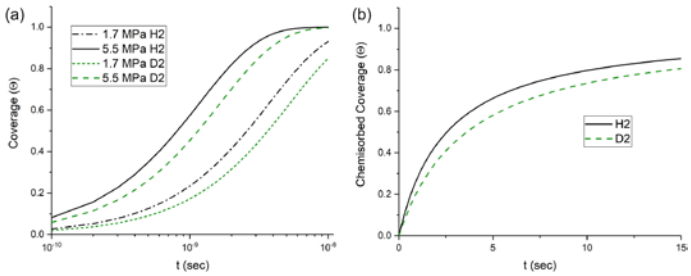

FIGURE 1: THE TEMPORAL DYNAMICS OF HYDROGEN AND DEUTERIUM ADSORPTION ON IRON (FE)

SURFACES UNDER HYDROGEN GAS PRESSURES OF 1.7 AND 5.5 MPA. PANEL (A) OF THIS FIGURE ILLUSTRATES THE RAPID ATTAINMENT OF FULL HYDROGEN ADSORPTION COVERAGE, OCCURRING WITHIN TENS OF NANOSECONDS. PANEL (B) FOCUSES ON THE CHEMISORPTION PROCESS OF HYDROGEN FROM ITS ADSORBED H_2 STATE.

2.3. DYNAMICS OF HYDROGEN PERMEATION WITHIN STEEL STRUCTURES

Following the adsorption, dissociation, and chemisorption of H_2 gas on the steel surface, the atomic hydrogen commences its diffusion through the steel matrix. Within the ferritic structure, hydrogen, owing to its small size, predominantly occupies interstitial spaces, particularly tetrahedral sites. This diffusion process is commonly represented through the application of Fick's law.

$$J = -D\frac{d[H]}{dx}, \qquad (9)$$

In this model, 'J' represents the hydrogen flux, 'D' denotes the diffusivity of hydrogen, and 'H' signifies the hydrogen concentration. In environments devoid of stress, the hydrogen concentration can be described using Sievert's Law [10]

$$[H]_0 = \frac{\Phi}{D}(P)^{1/2}, \qquad (10)$$

In this equation, 'Φ' symbolizes the hydrogen permeability, while 'P' refers to the pressure of hydrogen in the adjacent gaseous milieu. When subjected to hydrostatic stress, the stress-assisted hydrogen concentration, denoted as '$[H]_\sigma$', can be quantified by the following expression:

$$[H]_\sigma = [H]_0 e^{\sigma_h V/RT} = \frac{\Phi}{D}(P_H)^{1/2} e^{\sigma_h V/RT}, \qquad (11)$$

In this sophisticated model, 'σ_h' denotes the hydrostatic stress, 'R' represents the universal gas constant, and 'V', with a value of 2.0×10^{-6} m^{-3}/mol, signifies the partial molar volume of hydrogen in body-centered cubic (BCC) Fe [11]. At ambient temperature, the hydrogen permeability 'Φ' is quantified as 10^{13} atoms/m.s.MPa½ for hydrogen gas. Research has indicated that the energy associated with hydrogen trapping is not only responsive to hydrostatic stress but also to shear stress. Specifically, dislocations, characterized by high shear stress, are identified as zones of pronounced hydrogen accumulation, extending along the entire slip plane surrounding a dislocation core.

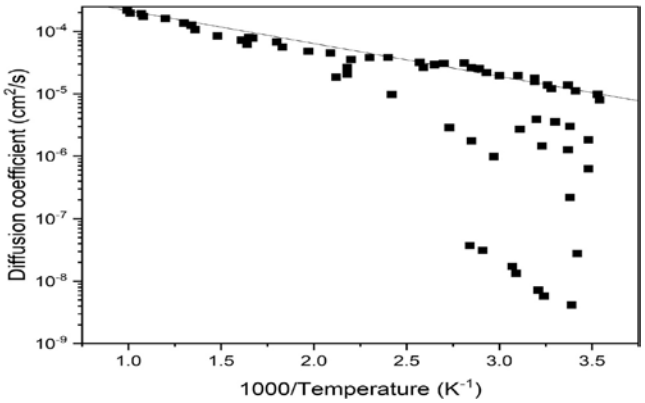

FIGURE 2. A COMPREHENSIVE COMPILATION OF DATA ON HYDROGEN DIFFUSIVITY IN IRON.

Hydrogen diffusion in iron, unlike in metals like nickel or vanadium, shows notable variability at room temperature, as depicted in Figure 2. At higher temperatures, diffusion aligns with an Arrhenius-type relationship, corroborated by ab initio calculations suggesting a diffusible hydrogen rate of around 10^{-5} cm^2/s at room temperature [12]. To explain slower diffusion rates observed at lower temperatures, the concept of hydrogen trap sites was introduced, indicating that hydrogen diffuses rapidly through iron but accumulates at microstructural defects like voids, dislocations, grain boundaries, and precipitates.

These traps vary in nature, with attractive traps altering hydrogen's diffusion path and physical traps randomly capturing it. The binding energy of these traps, determining their reversibility, is a crucial factor. Irreversible traps with high binding energies lock hydrogen below certain temperatures, while reversible traps with lower energies temporarily hinder but eventually allow hydrogen movement.

The behavior of hydrogen at grain boundaries depends on the boundary type; low-angle boundaries have interstitial sites similar to a bulk lattice, while high-angle boundaries exhibit higher binding energies. The role of grain boundaries as diffusion pathways is still debated, with studies showing mixed results based on boundary characteristics. Dislocations, acting as both attractive and physical traps, may facilitate 'short-circuit' diffusion paths and transport hydrogen under stress, creating unique hydrogen distribution patterns.

Vacancies also play a significant role, with hydrogen increasing vacancy formation and stabilizing vacancy clusters, and vice versa. This symbiotic relationship is crucial in understanding hydrogen behavior in iron.

The impact of trap sites on hydrogen embrittlement is complex. While they lead to high local hydrogen concentrations, critical in most embrittlement mechanisms, they also retard overall hydrogen diffusion. Irreversible traps could mitigate degradation by sequestering hydrogen away from sensitive areas. Identifying an optimal trapping energy balance, which slows diffusion without causing excessive hydrogen accumulation, is vital. This balance is key, as interactions that reduce diffusion rates also increase local solubilities,

determining a 'Goldilocks' trapping energy essential for optimizing hydrogen interaction with steel.

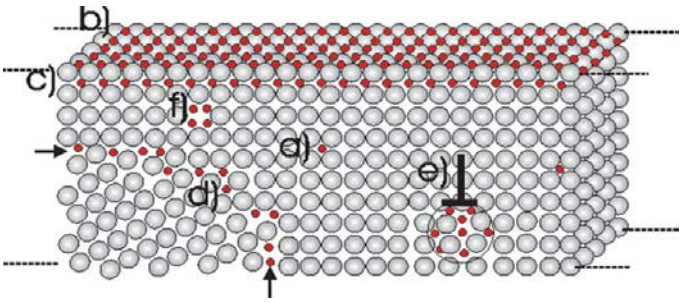

FIGURE 3. TRAP THEORY STATES THAT HYDROGEN AMASSES AT MICROSTRUCTURAL DEFECTS SUCH AS VOIDS, DISLOCATIONS, GRAIN BOUNDARIES, AND PRECIPITATES, WHICH IN TURN ACT AS TRAPS [13].

3. MECHANICAL PROPERTIES AND THEIR RELEVANCE IN HYDROGEN-RELATED APPLICATIONS

In engineering and scientific fields that are involved in designing components that interact with hydrogen or are engaged in studying the impact of hydrogen on materials, the comprehension of mechanical properties is crucial. These professionals scrutinize the intricate relationships among mechanical properties, microstructures, and processing techniques. The term 'hydrogen embrittlement' encompasses a range of phenomena, not limited to the reduction of area (RA) or decrease in elongation at failure, but extending to any deterioration of mechanical properties caused by hydrogen.

In the realm of design and material selection, key mechanical properties that are typically considered include reduction of area, elongation to failure, fatigue crack growth rate, fracture toughness, threshold for sustained load cracking, fatigue threshold, and stress life. Although yield strength and ultimate tensile strength (UTS) are fundamental properties for design considerations, their susceptibility to alteration by hydrogen, especially in its gaseous form, remains ambiguous, particularly in the context of smooth specimens composed of ferritic steels. This uncertainty underscores the need for a more nuanced understanding of how hydrogen interacts with different mechanical properties, to ensure the integrity and reliability of materials in hydrogen-influenced environments.

3.1. TENSILE TESTING

The impact of hydrogen on mechanical properties is pivotal in material design, influenced by factors such as loading conditions, test temperature, and hydrogen environment. Monotonic tensile testing provides critical insights into various properties like yield strength, ultimate tensile strength, and ductility [14]. It's noted that steel's susceptibility to hydrogen embrittlement, particularly in structural steels like those in pipelines, increases with its strength. However, this effect varies with the steel's microstructure. For instance, certain steel types exhibit reduced tensile strength under higher hydrogen pressures [15].

Notched tensile testing reveals significant reductions in yield and tensile strength, serving as a key tool for assessing hydrogen embrittlement susceptibility. This susceptibility is influenced by stress concentration and hydrogen concentration, modifiable by altering notch shapes. While reduction of area and elongation to failure in tensile tests are not used in the design, they are important for ranking materials' embrittlement susceptibility. In short, increasing hydrogen pressure typically leads to a decrease in elongation to failure, with yield strength showing no significant pressure-dependent variation. These observations are crucial for understanding the influence of hydrogen on material integrity, especially under high-pressure conditions.

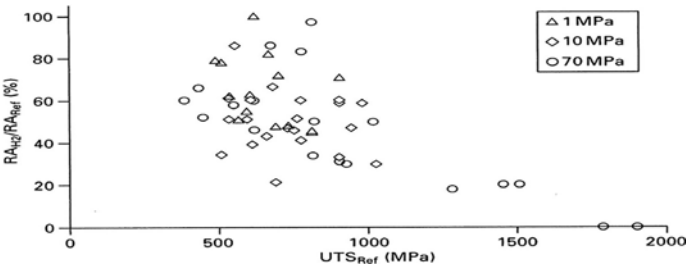

FIGURE 4. DEPENDING ON THE STRENGTH OF THE STEEL, HYDROGEN EMBRITTLEMENT, MEASURED AS THE RELATIVE REDUCTION OF THE AREA OF A SMOOTH SPECIMEN IN MONOTONIC TENSILE TESTING,

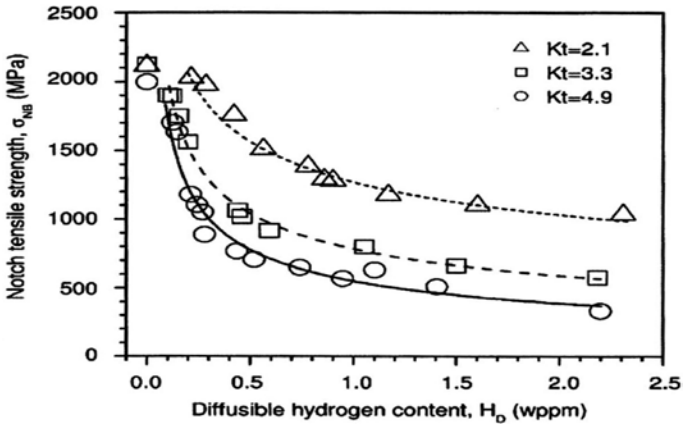

FIGURE 5. NOTCH TENSILE STRENGTH VS DIFFUSIBLE HYDROGEN CONTENT, IT HAS BEEN OBSERVED THAT NOTCHED SPECIMENS SHOW A SIGNIFICANT REDUCTION IN BOTH YIELD AND TENSILE STRENGTH [16].

3.2. ANALYSIS OF FRACTURE TOUGHNESS

The threshold stress intensity factor, K_{TH}, is a crucial parameter in fracture mechanics, representing the stress intensity below which crack propagation in hydrogen is unlikely. K_{TH} is

typically measured using a wedge-opening-load (WOL) test or a rising load test, with the former being displacement-controlled. These tests are particularly relevant for high-strength steels, where low fracture thresholds are observed. The rising load test, however, is applicable across a broader range of materials. K_{TH} is instrumental in the design of pressure vessels, as exemplified in the ASME Boiler and Pressure Vessel code.

For ferritic steels, K_{TH} tends to decrease with increasing hydrogen gas pressure or alloy strength, although the relationship with hydrogen pressure can be complex. For example, X100 steel shows a plateau effect in hydrogen's impact on K_{TH}, while DOT 3T steel exhibits only a minor decrease with increasing hydrogen pressure. Additionally, K_{TH}'s sensitivity to the initial load on the specimen increases as the steel's strength decreases. Fracture toughness testing in hydrogen typically mirrors the trends observed in the measurement of the threshold stress intensity factor. Common properties reported include K_{IC}, J_{IC}, crack growth resistance (J–R curves), or dJ/da. Fracture toughness is notably lower in hydrogen gas compared to air or inert environments, with the toughness in the air often being at least double that in hydrogen at pressures above 5.5 MPa [17]. Although fracture toughness generally decreases with increasing hydrogen pressure, the pressure sensitivity varies.

Alvarez et al.'s study on the impact of displacement rate on the fracture toughness of C–Mn structural steel and quench and tempered (ferrite-martensite) steel, pre-charged with hydrogen, revealed that toughness decreases with a reduction in the displacement rate of the test. This effect was more pronounced in ferrite-martensite steel. In many instances, fracture toughness does not correlate directly with yield strength [18], and while some studies indicate a relationship between increased alloy strength and decreased fracture toughness, this trend is mostly observed in very high-strength alloys.

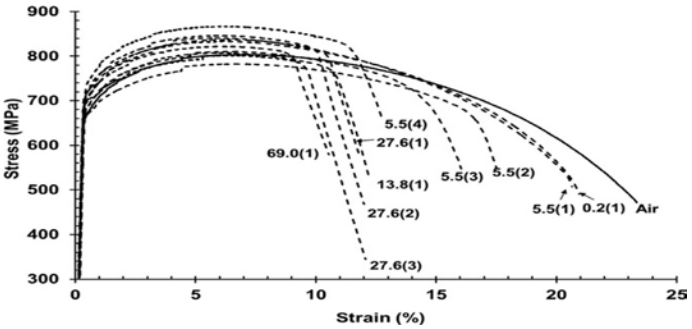

FIGURE 6. TENSILE CURVES FROM LONGITUDINAL X100 STEEL SPECIMENS TESTED IN HYDROGEN AT DIFFERENT GAS PRESSURES AND A STRAIN RATE OF $7*10^{-3}$ S^{-1}.

TABLE 1. Tensile data from longitudinal X100 steel specimens at a strain rate of $7*10^{-3}$ s^{-1}, σy 0.2% =yield strength, UTS = ultimate tensile strength, Ef = elongation at failure, and RA = reduction of area (final area/original area) [15].

Gas	Pressure (MPa)	$\sigma_{y\,0.2\%}$ (MPa)	UTS (MPa)	E_f (%)	RA (%)
Air	~0.08	665	792	21	75
Air	~0.08	674	804	23	78
Air	~0.08	698	810	22	75
Average		679	802	22	76
Standard deviation		17.1	9.2	1.0	1.9
H_2	0.2	719	834	21	68
H_2	5.5	747	867	11	24
H_2	5.5	685	811	16	28
H_2	5.5	670	783	18	39
Average		701	820	15	30
Standard deviation		40.8	42.8	3.2	7.8
H_2	13.8	693	808	11	19
H_2	27.6	704	803	9	28
H_2	27.6	707	837	11	21
H_2	27.6	731	846	12	20
Average		714	829	11	23
Standard deviation		14.8	22.7	1.3	4.2
H_2	69.0	715	823	9	16

3.3. ANALYSIS OF FATIGUE PROPERTIES

Fatigue crack growth rate (FCGR) testing is a fundamental tool in predicting the remaining lifetime of structures like pipelines and pressure vessels, given an initial flaw size. It's also essential in fracture-mechanics-based design, as employed in standards like the ASME Boiler Pressure Vessel code and the ASME B31.12 Hydrogen Piping and Pipelines code [20]. Key variables influencing FCGR testing include the stress intensity range (ΔK), loading frequency, and hydrogen gas pressure. Other factors like load waveform, stress ratio, steel strength, and microstructure also play roles in affecting FCGR.

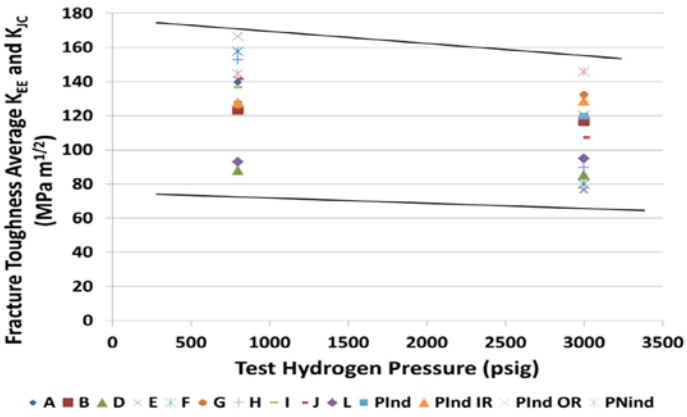

FIGURE 7. FRACTURE TOUGHNESS OF FERRITIC STEELS AS A FUNCTION OF HYDROGEN GAS PRESSURE. (3000 PSIG = 21 MPA).

Load waveform slightly impacts hydrogen-assisted fatigue crack growth rate (HA-FCGR), particularly at low-stress ratios. The stress ratio affects the onset of crack acceleration and the stress level for the onset of stage III FCGR [21]. Steel strength, interestingly, does not generally correlate with HA-FCGR. Studies have shown no consistent relationship between yield strength and HA-FCGR across different ferritic steels.

Microstructure's impact on HA-FCGR is complex and may depend on dominant experimental factors such as ΔK, loading frequency, and gas pressure.

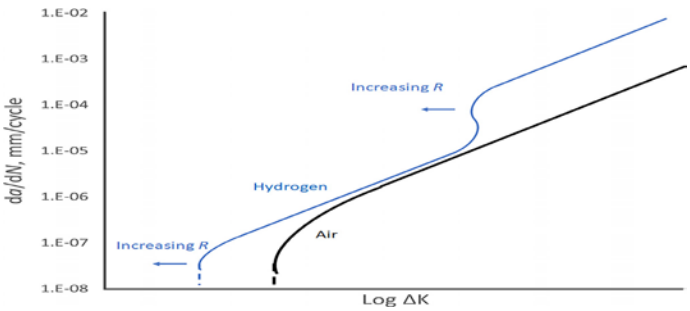

FIGURE 8. DIAGRAM OF THE EFFECT OF STRESS RATIO ON THE HA-FCGR.

FCGRs typically increase significantly in hydrogen environments compared to air or inert environments. The effect of hydrogen gas pressure on HA-FCGR varies, with plain carbon ferritic steels generally showing an increase in FCGR with rising hydrogen pressure. However, some studies indicate little pressure dependence on HA-FCGR across a range of ferritic steels. At high-stress intensity factors, ferritic steels tend to converge to similar HA-FCGRs regardless of hydrogen pressure.

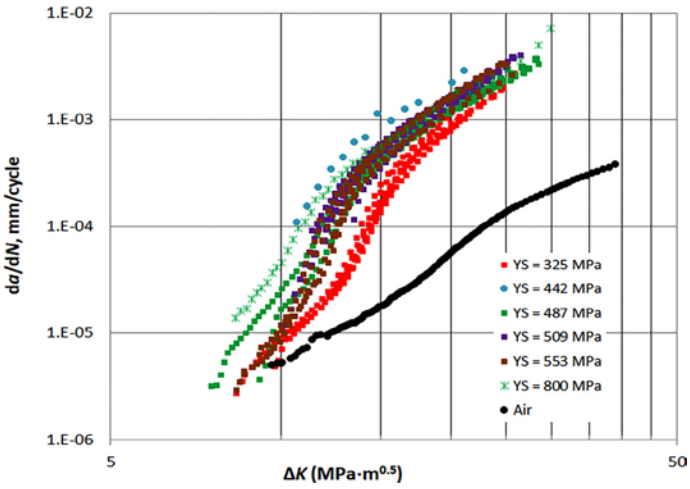

FIGURE 9. HA-FCGR AT A HYDROGEN GAS PRESSURE OF 5.5 MPA, LOADING FREQUENCY OF 1 HZ, AND STRESS RATIO OF 0.5 FOR PIPELINE STEELS WITH YIELD STRENGTHS RANGING FROM 325 MPA TO 800 MPA [21].

The loading frequency's impact on HA-FCGR is generally minimal, though some variability is observed across different steels, which can be attributed to differences in microstructure and hydrogen trapping. In summary, while FCGRs are markedly higher in hydrogen environments, the specific effects of factors like gas pressure, loading frequency, and microstructure can vary, necessitating a tailored approach for each material and application.

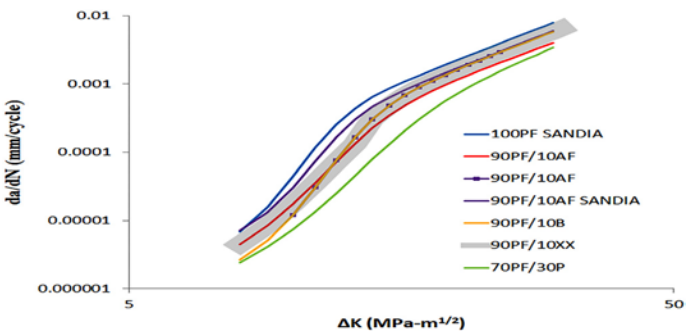

FIGURE 10. HA-FCG OF PIPELINE STEELS WITH VARYING AMOUNTS OF POLYGONAL FERRITE (PF) TESTED AT A HYDROGEN GAS PRESSURE OF 5.5 MPA, [22].

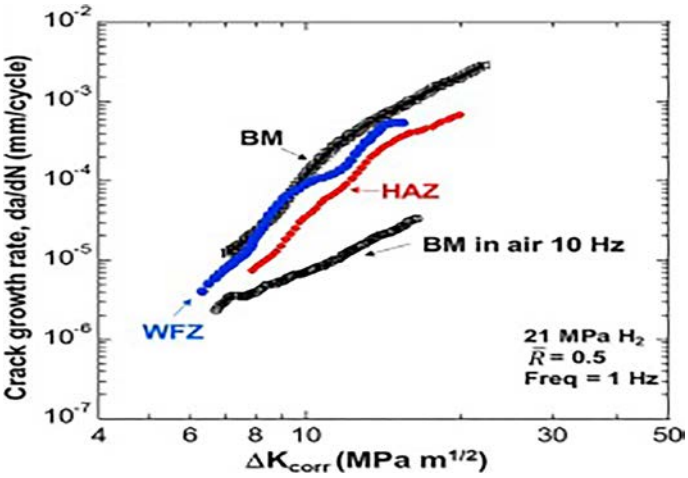

FIGURE 11. FCGR FOR AN X100 PIPELINE STEEL, WELD, AND HEAT-AFFECTED ZONE, CORRECTED FOR RESIDUAL STRESS [23].

3.4. EVALUATION OF WELD PERFORMANCE

In ferritic steels, welds require special consideration due to their susceptibility to hydrogen embrittlement, often exacerbated by inclusions and varied microstructures resulting from welding processes. The intense localized heating, cooling rates, and the presence of impurities like carbon and sulfur during welding can lead to a range of secondary phases and microstructures, which might be more prone to hydrogen embrittlement. The age of the weldment significantly influences its characteristics; newer welds generally exhibit cleaner microstructures with finer, more uniform grain sizes compared to older welds, which often contain more inclusions and pearlite.

Welds typically feature higher aspect ratio ferrite grains and greater variation in grain size than base metals. Common microstructures in welds include Widmanstätten ferrite, acicular ferrite, and allotriomorphic ferrite along austenite grain boundaries. Friction stirs welds, formed from the base metal, usually have finer grains but may contain more carbides.

Electrical resistance welds (ERWs) closely resemble the base metal, barring significant void formation.

The heat-affected zone (HAZ) surrounding welds, due to heating and cooling from the welding process, exhibits gradient microstructures. The HAZ in older steels can range from variously tempered martensite near the fusion zone to degenerated pearlite closer to the base metal, with significant variations in grain size.

Mechanical testing of welds in hydrogen environments, predominantly FCGR testing, indicates that modern welds (from the 2000s onward) perform similarly to base metals in hydrogen. However, factors like inclusions and residual stresses may significantly impact crack growth rates. While extensive research has been conducted on austenitic steel welds in hydrogen, studies on ferritic steel welds are less common. Research on X70 steel pipes, for instance, showed comparable fracture toughness between welds and base metal. Similarly, testing and modeling of HAZs in X52 and X70 pipes revealed that the base metals were at least as susceptible to hydrogen as the heat-affected zones.

3.5. ANALYSIS OF FAILURE MECHANISMS

While the primary emphasis of this review is on ferritic steels, the discussion of hydrogen embrittlement mechanisms inevitably encompasses studies on a broader range of materials. Most experts concur that considering hydrogen's widespread impact on various structural materials, any proposed mechanism for hydrogen embrittlement should have universal applicability. Consequently, numerous studies have been conducted on model materials like nickel, often complemented by subsequent research confirming similar effects in body-centered cubic (BCC) materials. Thus, while our focus remains predominantly on ferritic steels, findings from other materials are also referenced to provide a comprehensive understanding. For those interested in a more in-depth exploration, several detailed reviews on specific mechanisms and their historical development are mentioned in relevant sections.

3.5.1. ANALYSIS OF HYDROGEN-INDUCED DECOHESION

The hydrogen-enhanced decohesion (HEDE) theory, one of the oldest and most established mechanisms in the study of material embrittlement, was initially proposed by Troiano in 1960. This theory posits that dissolved hydrogen reduces the cohesive strength of metal bonds, leading to bond rupture at lower stresses. HEDE is broadly categorized into two types: lattice decohesion and boundary decohesion.

In boundary decohesion, hydrogen accumulation at grain boundaries or around secondary phases like carbides in steels weakens the cohesive strength, resulting in material failure. This phenomenon is particularly evident in materials like nickel, where hydrogen aging at grain boundaries leads to significant intergranular fracture. In dissimilar metal welds, hydrogen-assisted boundary failure can manifest in unexpected ways, such as "cleavage-like" failure through carbide precipitates. The role of elements like carbides in hydrogen embrittlement is debated; they can act as either hydrogen sinks or fracture initiation sites.

In ferritic steels, intergranular failure due to hydrogen is less common compared to FCC austenitic alloys or nickel-based alloys. It typically occurs under aggressive electrochemical charging or fatigue conditions. However, to induce a meaningful reduction in boundary cohesive strength, calculations suggest that high hydrogen pressures are necessary, implying that other contributing factors are involved in intergranular failure.

The lattice decohesion aspect of HEDE, where hydrogen is thought to weaken the lattice cohesion, is more contentious. In ferritic steels, the presence of hydrogen can shift failure modes from ductile to brittle-like trans-granular failure under certain conditions [24]. This effect is likened to a ductile-to-brittle transition dependent on hydrogen concentration rather than temperature. Atomistic modeling proposes several mechanisms for hydrogen-induced brittle fracture, such as the formation of a brittle “nano hydride” phase at the crack tip or suppression of dislocation emissions.

While HEDE's simplicity and the brittleness of failure make it a compelling model, a fully predictive understanding of its mechanism remains elusive. The challenge lies in the lack of direct measurements of hydrogen's impact on cohesive strength, with only first-principles calculations currently available. These calculations, though insightful, may not fully quantify the effects in real materials.

3.5.2. ANALYSIS OF HYDROGEN-INDUCED LOCALIZED PLASTICITY

The hydrogen-enhanced localized plasticity (HELP) model, developed in the 1980s and 1990s by Birnbaum, Robertson, Sofronis, and colleagues, suggests that hydrogen influences dislocation behavior in metals, including iron [25]. This theory, supported by meticulous transmission electron microscopy (TEM) studies, notes increased dislocation velocity and closer dislocation spacing in the presence of hydrogen, along with reduced cross-slip and a slight decrease in stacking fault energy. The model proposes that hydrogen forms an atmosphere around dislocations, altering their interaction with obstacles like grain boundaries and secondary phases, thus impacting the material's plasticity.

While some studies indicate hydrogen can cause softening in high-purity iron, this effect varies with temperature, suggesting a connection between hydrogen-enhanced plasticity and embrittlement within certain temperature and strain-rate ranges. Increased relaxation rates observed in stress relaxation tests further imply heightened dislocation mobility in the presence of hydrogen.

One challenge in understanding HELP is reconciling increased local plasticity with the globally brittle behavior observed in materials. Recent research has explored the microstructure beneath hydrogen-induced fracture features, revealing extensive plastic deformation, contradicting the brittle appearance of the fracture surfaces. This suggests accelerated plasticity occurs not just at the fracture surface but throughout the strained material.

The impact of hydrogen on dislocation motion, such as increased mobility and packing or decreased cross-slip, leads to changes in microstructural development with strain. These changes include higher dislocation density and altered dislocation organization, potentially influencing failure mechanisms. The distribution of hydrogen associated with dislocation movement could also differ from classical diffusion models. Despite ongoing debates about the exact mechanisms by which hydrogen influences dislocation motion, the consensus is that hydrogen does affect dislocation behavior and microstructural evolution, which are crucial factors in material failure under hydrogen exposure.

3.6. ANALYSIS OF HYDROGEN-ENHANCED STRAIN-INDUCED VACANCY FORMATION

The role of increased vacancy generation in the presence of hydrogen, crucial to understanding embrittlement mechanisms, is primarily attributed to Nagumo and colleagues. Their research, using techniques like thermal desorption spectroscopy (TDS), revealed a significant surplus of vacancies in iron when deformed in a hydrogen environment. This phenomenon, characterized by vacancy concentrations vastly exceeding equilibrium levels, has been observed by other researchers and in various materials.

First-principles calculations suggest that hydrogen's interaction with vacancies lowers their formation energy, leading to these elevated concentrations. TDS studies identified these trap sites as vacancies, distinguishable from other microstructural defects due to their removal at lower annealing temperatures. Positron annihilation spectroscopy further supports this finding, as it can detect vacancies by analyzing the mean lifetimes of trapped positrons in the material.

The association between vacancies and embrittlement is evident in experiments combining tensile straining and heating. Materials like iron or Inconel 625, pre-strained in hydrogen, show reduced ductility, partially recoverable through hydrogen release but fully recoverable only after higher-temperature aging that removes hydrogen-vacancy complexes.

The concept of nano-void coalescence (NVC) has been proposed to describe the embrittlement mechanism, where vacancy clusters evolve into nano-voids under intense strain, leading to failure similar to microvoid coalescence in traditional ductile fractures. However, it's important to note that this theory is not universally accepted, as some studies under similar conditions do not find evidence of nanovoids.

Overall, the evidence strongly suggests that vacancies play a significant role in hydrogen embrittlement, particularly through their interactions with dislocations. Accelerated dislocation activity in hydrogen environments leads to increased vacancy formation, which in turn influences grain boundaries and dislocation behavior, potentially contributing to the observed differences in microstructure during deformation with hydrogen.

3.7. ANALYSIS OF HYDRIDE FORMATION AND PHASE TRANSFORMATIONS

Hydride formation and cleavage is a recognized mechanism of embrittlement, particularly relevant to hydride-forming materials like Group Vb metals (vanadium, niobium, tantalum), titanium, zirconium, and their alloys. In these materials, low hydrogen solubility leads to the formation of a brittle hydride phase, which cleaves along crystallographic planes under stress. Additionally, crack tip stresses may induce hydride precipitation, with the hydride's morphology influencing the crack direction.

In other metallic systems, such as nickel, metal hydrides can form under high stress or hydrogen fugacity conditions, typically in aggressive charging environments. These hydrides are generally metastable. Some studies propose the formation of nano hydrides ahead of crack tips, but this theory requires further validation, as observed failure modes in materials like nickel and ferritic steels do not consistently align with this model.

In austenitic stainless steels, hydrogen can facilitate the formation of martensitic phases, though the significance of this transformation about hydrogen embrittlement remains debated. Unlike austenitic or martensitic steels, ferritic steels, more stable over the temperature range of hydrogen embrittlement, do not exhibit this phase transformation mechanism.

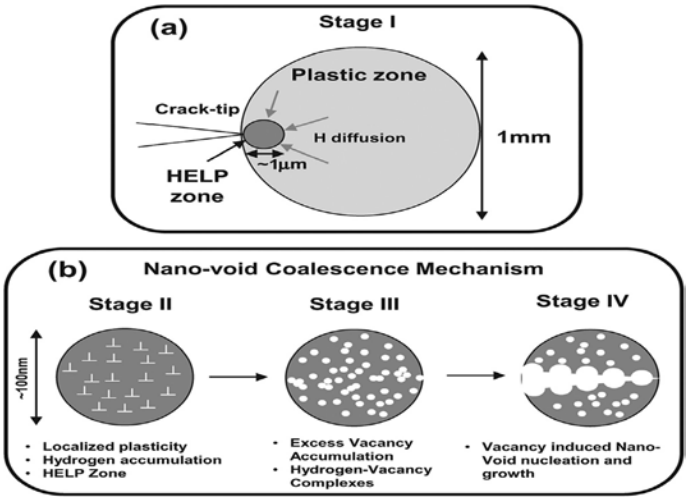

FIGURE 12. SCHEMATIC OF A NANO-VOID COALESCENCE MODEL [24].

3.8. ANALYSIS OF THE DEFACTANT THEORY

The "Defactant" concept, introduced by Kirchheim and colleagues, represents a thermodynamic framework focused on solute-defect interactions, particularly relevant to hydrogen embrittlement. This theory suggests that hydrogen, akin to surfactants on surfaces, acts on defects to reduce their formation energy. The term "Defactant" is derived from the analogy with "Surfactant", signifying a DEFect ACTing AgeNT. According to this concept, the higher the chemical potential of hydrogen, the more pronounced its effect.

This approach can be viewed as an alternative perspective to traditional trapping theory. Instead of focusing solely on how hydrogen atoms reduce energy by occupying lower energy trapping sites, the Defactant theory considers the energy gain for the defect trap in capturing hydrogen. Consequently, this concept

implies that hydrogen stabilizes vacancies, corroborating findings associated with vacancy mechanisms. Additionally, it suggests an increase in dislocation motion, particularly in body-centered cubic (BCC) metals, by facilitating double kink formation and reducing the line energy of dislocations, thereby supporting observations related to the HELP mechanism.

The Defactant mechanism can be seen as encompassing various aspects of previously described mechanisms, with the interplay between hydrogen's chemical potential and the availability of defects determining the predominant effect. While the current formulation of this model does not offer predictive capabilities regarding the dominant condition, it could be further refined by incorporating kinetic considerations to enhance its applicability and explanatory power in the context of hydrogen embrittlement.

3.9. ANALYSIS OF COMBINED EMBRITTLEMENT MECHANISMS

The concept of multiple embrittlement mechanisms operating concurrently has gained acceptance in recent times, acknowledging that various mechanisms may interact under different conditions to cause embrittlement. A notable study by Novak et al. proposed a model where a dislocation pileup at a grain boundary precipitate leads to interface decoherence and subsequent crack formation.

In the context of intergranular failure, materials and conditions vary significantly. For instance, studies on nickel have demonstrated that prolonged hydrogen aging increases the incidence of intergranular failure, indicating that sufficient hydrogen accumulation at grain boundaries can lead to brittle failure with minimal strain. However, in dynamic scenarios where hydrogen doesn't accumulate as much, intergranular failure still occurs. In iron, such failure is condition-specific; atomistic modeling suggests that hydrogen reduces the cohesive strength of grain boundaries based on external H2 gas pressure, but substantial pressure is required to induce intergranular failure, pointing to the involvement of additional mechanisms.

Investigations into the microstructure beneath intergranular fracture surfaces in iron and nickel revealed highly developed dislocation structures, suggesting strains much larger than those at failure. This extensive dislocation structure, existing beyond the immediate vicinity of the fracture surface, implies that this isn't merely a crack tip concentration effect. The HELP mechanism's influence on dislocation structure development leads to accelerated deformation, impacting dislocation-grain boundary interactions. These interactions may distort the grain boundary and hydrogen deposition, thus reducing its cohesive strength. This reduction is critical to intergranular failure, but it wouldn't occur without HELP-accelerated deformation.

In martensitic steels, similar observations were made, where "quasi-cleavage" failures were martensitic lath boundary failures, influenced by extensive dislocation activity in shear bands. These connections between different mechanisms suggest that embrittlement is a complex, multifaceted process, with further research needed to fully understand the interplay of these mechanisms.

4. ADVANCES AND INSIGHTS IN RECENT DEVELOPMENTS

For over a century, the adverse impact of hydrogen on the physical properties of iron and steel has been recognized. Despite extensive research, significant questions about the structure-property-performance relationships in steels affected by hydrogen embrittlement, particularly ferritic steels, remain unresolved. This is partly due to the unique challenges associated with these steels, including their high diffusivities and low solubilities for hydrogen. These characteristics often result in specimens exhibiting in-air properties soon after removal from a hydrogen environment.

Recent efforts have concentrated on developing specialized test chambers for in situ mechanical testing using neutron and X-ray measurements in gaseous hydrogen environments. However, direct observation of hydrogen in structural materials faces several experimental challenges, including limitations in spatial and temporal resolution and the prevalence of background hydrogen in high vacuum environments.

To address these challenges, significant work has been directed toward high-resolution spectroscopy, microscopy, and atom probe tomography (APT) of ferritic steels post-hydrogen testing. These techniques focus on assessing hydrogen content, distribution, and binding states, as well as differentiating between environmentally-derived background hydrogen and hydrogen introduced during testing.

This section will summarize recent advances and insights gleaned from in situ tests and high-resolution measurements. For further information on other prevalent methods for detecting hydrogen in steels, such as thermal desorption spectroscopy (TDS), Ag reduction/decoration, hydrogen imprint technique, and neutron radiography, readers are referred to a recent comprehensive review and related references.

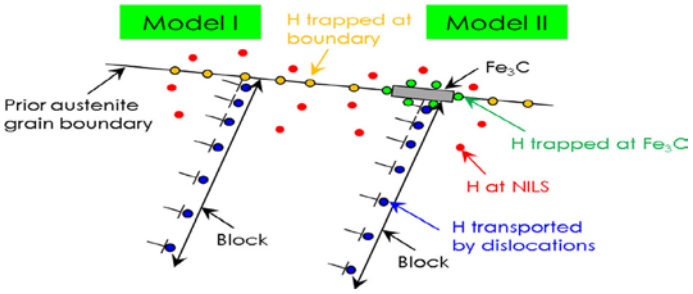

FIGURE 13. SCHEMATIC OF HELP-ASSISTED DECOHESION IN MARTENSITIC STEEL [26].

4.1. ADVANCES IN IN SITU MECHANICAL TESTING

Connolly et al. developed a sophisticated gas pressure chamber specifically for in situ mechanical testing of steel specimens under neutron scattering and X-ray diffraction. This chamber, crafted from monolithic 6061-T6 aluminum with a 3.175mm wall thickness, was designed to address not only safety concerns associated with gas pressure but also to ensure transparency to neutrons and X-rays. Utilizing this chamber, they conducted neutron-diffraction-based strain mapping near fatigue crack tips in X70 steel C(T) samples in both hydrogen and air

environments. The strain maps revealed that hydrogen amplifies crack-tip elastic strain under a given load more than in air, aligning with the Hydrogen Enhanced Decohesion (HEDE) theory.

Additionally, the chamber facilitated synchrotron X-ray diffraction measurements in AISI 4130 steel, allowing for an analysis of strain components and dislocation density near fatigue crack tips in air and hydrogen. These findings indicated differences in dislocation density profiles in air versus hydrogen, supporting the Hydrogen Enhanced Localized Plasticity (HELP) mechanism. The combined results from neutron scattering and X-ray diffraction studies suggest a synergy between HEDE and HELP mechanisms, driven by increased hydrogen concentration through HELP.

Beyond X-ray and neutron diffraction, quasi-elastic neutron scattering offers insight into hydrogen diffusion coefficients in different microstructural components. Inelastic scattering could shed light on hydrogen's effects on the atomic bonding of host metals, an area primarily understood through first-principles modeling. Neutron imaging, which focuses on neutron beam attenuation, proves particularly effective in mapping hydrogen concentrations.

The potential of these techniques in understanding hydrogen embrittlement hinges on continued innovative research efforts, particularly in integrating measurements like in situ mechanical testing with strain mapping.

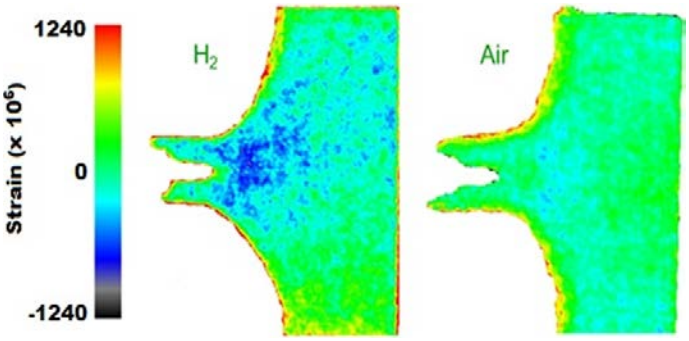

FIGURE 14. STRAIN MAPPING OF AN X70 STEEL C(T) SAMPLE UNDER MECHANICAL LOAD IN BOTH HYDROGEN AND AIR BY NEUTRON SCATTERING [9].

4.2. ADVANCED HIGH-RESOLUTION MICROSCOPY TECHNIQUES

The challenge of linking macroscale mechanical responses to nanoscale microstructural changes has been advanced by recent progress in microscopy technologies. This advancement enables the correlation of effects across various length scales, previously unfeasible. For example, Bertsch et al. demonstrated that higher dislocation density observed in TEM due to hydrogen loading manifested differently in larger-scale SEM measurements, suggesting increased plasticity at a finer scale but appearing as reduced plasticity at a coarser scale.

High-resolution techniques like SEM, TEM, and AFM have been crucial in understanding hydrogen-assisted fracture mechanisms. Martin et al., for instance, examined different morphologies of hydrogen-induced fracture surfaces in ferritic steels. By utilizing FIB machining to extract samples directly from fracture surfaces, they correlated surface features with sub-surface microstructural characteristics. Their findings revealed distinct morphologies and associated microstructural changes beneath the fracture surfaces, challenging the notion of purely brittle fracture processes in the presence of hydrogen.

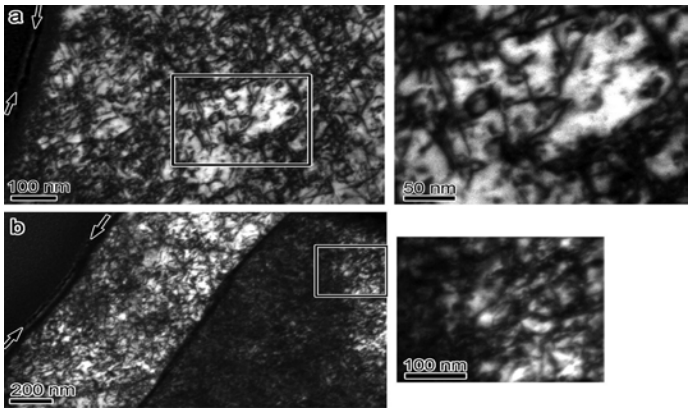

FIGURE 15. TEM IMAGES OF THE MICROSTRUCTURE AND DISLOCATION DENSITY BELOW THE HYDROGEN-INDUCED “FLAT” FRACTURE SURFACE IN FERRITIC STEEL [27].

Similar studies, like those conducted by Wang et al., have observed more plasticity beneath fracture surfaces than expected, suggesting a more advanced microstructure development in the presence of hydrogen. This observation has been supported by studies in various materials like nickel, martensitic steels, and austenitic stainless steels. FIB machining has also facilitated the creation of small-scale samples for in situ studies, enabling tests like nanopillar compression and micro-cantilever fracture toughness to gain insights into material behaviors under hydrogen exposure.

Additionally, scanning Kelvin probe force microscopy (SKPFM) has emerged as a sensitive tool for detecting hydrogen in metals, with applications in studying diffusion behaviors in different steel phases. Krieger et al. combined SKPFM with TDS and electron microscopy to analyze hydrogen trapping sites in ferritic steel, offering a more nuanced understanding of different traps.

Overall, the integration of advanced microscopy techniques has significantly enhanced our understanding of hydrogen's interaction with materials. While some results confirm existing theories, the ability to directly observe and measure these phenomena marks a substantial advancement in the field.

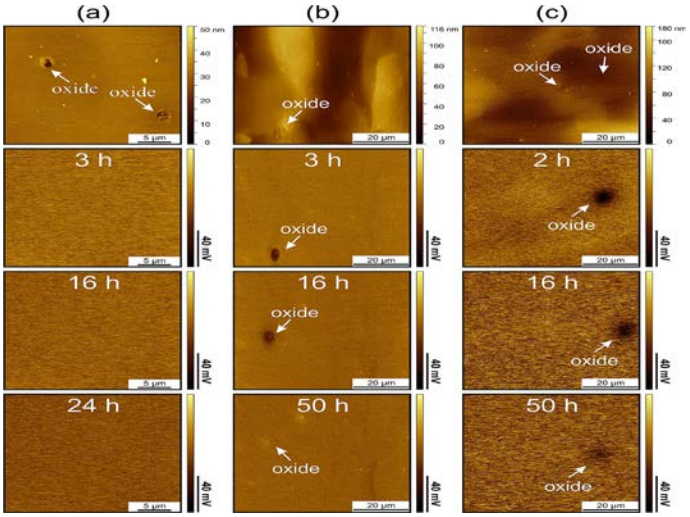

FIGURE 16. TOPOGRAPHY (TOP ROW) AND SKPFM (BOTTOM THREE ROWS) IMAGES OF (A) ANNEALED, (B) COLD ROLLED, AND (C) RECRYSTALLIZED FERRITIC STEEL AS A FUNCTION OF TIME [28].

4.3. HIGH-RESOLUTION SPECTROSCOPY

Recent advancements in secondary ion mass spectrometry (SIMS) are promising for pinpointing the exact location of hydrogen within metal microstructures. Early studies by Takai et al. used SIMS to identify hydrogen and deuterium trapping sites in high-strength steel. Despite debates over deuterium's comparability to hydrogen, its similar chemical properties make it a valuable tracer. The study measured significantly higher hydrogen ion counts at non-metallic inclusions, grain boundaries, and segregation bands compared to the matrix. Further SIMS analysis showed variations in deuterium distribution and desorption in ferrite and pearlite, suggesting differences in trapping between these microstructures.

Recent advancements have focused on reducing diffusivity through cryogenic testing and enhancing lateral resolution in SIMS. Nishimoto et al. conducted SIMS studies at 83 K, revealing that hydrogen-charged specimens exhibited significantly higher hydrogen secondary ion intensity than uncharged ones, a finding only possible at cryogenic temperatures.

Sobol et al. employed time-of-flight SIMS (ToF-SIMS) combined with electron microscopy for deuterium-assisted cracking studies in duplex stainless steel, achieving lateral resolutions of approximately 100 nm. ToF-SIMS data indicated different deuterium yields in austenite and ferrite grains, contributing to cracking and delamination.

McMahon et al. utilized nanoscale SIMS (NanoSIMS) to explore deuterium distributions in stainless steel after fatigue tests, achieving a finer lateral resolution of around 50 nm. This enabled imaging near crack tips and inclusions, suggesting that dislocation tangles and inclusions are deuterium trap sites. A logical progression for SIMS in ferritic steels is the combination of cryogenic conditions with NanoSIMS to enhance the understanding of hydrogen embrittlement mechanisms in these materials.

However, a limitation of SIMS is its inability to provide crystallographic or microstructural information. Complementary techniques like etched surface imaging, electron channeling contrast imaging, or electron-backscattered diffraction mapping can offer additional insights, creating a more comprehensive picture of hydrogen distribution in complex steel microstructures.

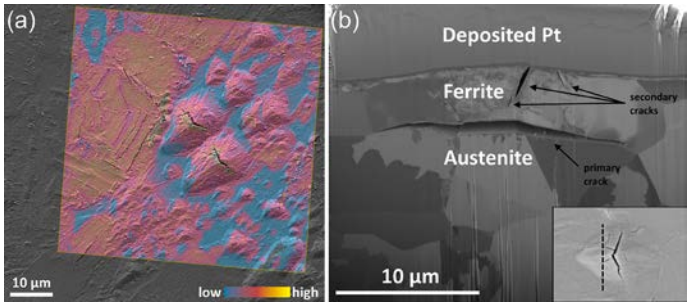

FIGURE 17. (A) SEM TOPOGRAPHIC IMAGE AND TOF-SIMS PC1 DEUTERIUM DATA FOR DUPLEX STAINLESS STEEL. THE ARROWHEAD-SHAPED PLATES REVEAL CRACKS AND MICRO TWINS WITH SIGNIFICANTLY HIGHER DEUTERIUM CONCENTRATIONS. (B) SECONDARY ION CROSS-SECTIONAL PROFILE FOR ONE SUCH PLATE [29].

4.4. ADVANCED HIGH-RESOLUTION TOMOGRAPHY TECHNIQUES

Recent advancements in atom probe tomography (APT) have focused on reducing deuterium diffusivity and enhancing lateral resolution, positioning APT as a pioneering method for atomic-scale imaging and chemical composition analysis. In APT, deuterium often substitutes for hydrogen, providing insights into hydrogen behavior within metals. Gemma et al. conducted a significant APT study on Fe/V films, highlighting the importance of controlling analysis temperature to accurately measure deuterium concentrations, especially in materials like ferritic steels. Takahashi et al. further developed APT applications by investigating deuterium profiles in TiC precipitation-hardening ferritic steel. They found that deuterium atoms concentrated along the broad surfaces of TiC platelets, suggesting trapping sites related to carbon vacancies or misfit dislocations at the TiC-matrix interface.

Subsequent research by Takahashi et al. on vanadium carbide (VC) precipitation in ferritic steels revealed deuterium atoms in and around VC platelets, depending on their size. This led to a hypothesis that misfit dislocation cores were trapping sites, later revised based on further studies showing changes in C/V stoichiometry and a lack of misfit dislocations.

Chen et al. used APT to investigate hydrogen trapping in ferritic steels with carbide precipitates. Their findings indicated a correlation between deuterium atoms and trapping sites, with a statistical approach revealing that deuterium was restricted to the

interior of carbides, contrasting earlier work on VC-precipitation steels.

APT's high-resolution capabilities make it an effective tool for studying hydrogen trapping in ferritic steels, particularly in dislocations, grain boundaries, and precipitates. However, APT's limited detection rate of atoms means it cannot detect microstructural defects like grain boundaries and dislocations directly. Chemical segregation of secondary elements can serve as proxies for certain microstructural features, but this approach has limitations in capturing the full spectrum of microstructural characteristics.

The combination of TEM imaging and APT analysis could offer a more comprehensive understanding of chemical segregation at microstructural features. TEM's similar chemical spatial resolution and ability to image defects by diffraction contrast complement APT's capabilities, paving the way for more detailed insights into hydrogen behavior in ferritic steels.

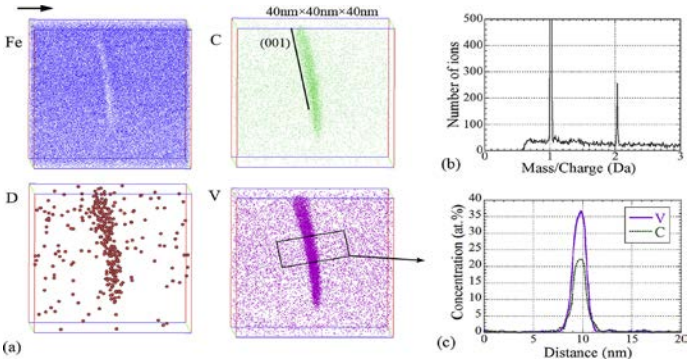

FIGURE 18. (A) APT ELEMENTAL MAPS AND (B) MASS-TO-CHARGE SPECTRUM OF A DEUTERIUM-CHARGED VC-PRECIPITATION FERRITE STEEL AGED FOR 8 H. THE DEUTERIUM ATOMS ARE DISTRIBUTED ALONG THE BROAD SURFACE OF THE PLATELET. (C) THE CONCENTRATION PROFILES OF CARBON AND VANADIUM [30].

5. SUMMARY AND FUTURE PERSPECTIVES

Hydrogen embrittlement's complexity, stemming from varied hydrogen-metal interactions, requires diverse techniques for thorough understanding. Significant progress, particularly in the last decade, is attributed to new experimental methods validating theories like hydrogen trapping, enhancing confidence in mechanism modeling. The integration of different investigative techniques is a key trend for future development.

Yet, challenges remain, especially in identifying hydrogen's precise location in metals and its impact on bonding. These are critical for a complete understanding of embrittlement mechanisms. Advanced techniques like APT, SIMS, and neutron diffraction are promising but face challenges, particularly in ferritic steels due to high hydrogen diffusion rates.

Simulations need to accurately represent real-world conditions, including temperature, strain rate, and concentration ranges relevant to hydrogen embrittlement. The ultimate goal is to improve the prediction of steel lifespans in hydrogen service and inform new material development, shifting from phenomenological to physics-based modeling that incorporates microstructure-specific data.

Future efforts should focus on measurements that can distinguish between different microstructural features, using innovative sample design or data deconvolution. Mechanical property testing must also evolve to more accurately reflect actual service conditions. Predictive models require data across multiple scales to understand the properties and behaviors of micro and nano-constituents. As the need for hydrogen infrastructure increases, advancements in the field are anticipated, leading to accurate predictions of hydrogen-induced behavior and smarter material design and selection.

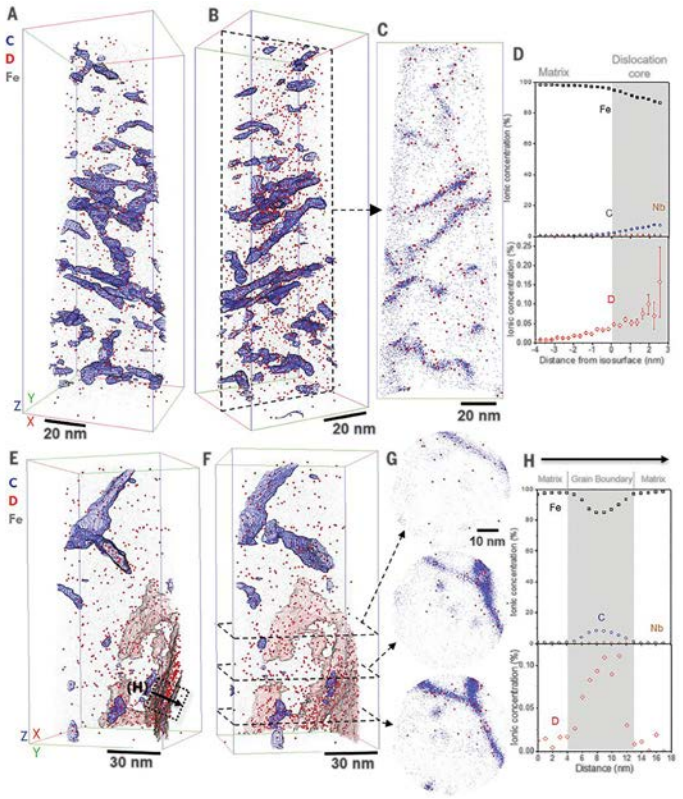

FIGURE 19. APT ANALYSES OF DEUTERIUM-CHARGED MARTENSITE STEEL [31].

REFERENCES

[1] Moradi, R.; Groth, M.K. Hydrogen storage and delivery: Review of the state of the art technologies and risk and reliability analysis. *Int. J. Hydrog. Energy* **2019**, *44*(23) 12254-12269.

[2] Li, X.; Ma, X.; Jhang, J.; Akiyama, E.; Wang, Y.; Song, X. Review of Hydrogen embrittlement in metals: Hydrogen diffusion, Hydrogen characterization, Hydrogen embrittlement mechanism and prevention. *Acta Metallurgica Sinica* **2020**, *33*, 759-773.

[3] Louthan, M. R.; Hydrogen embrittlement of metals: A primer for the failure analyst. *J Fail. Anal. And Preven.* **2008**, *8*, 289-307.

[4] Barrera, O.; Bombac, D.; Chen, Y.; Daff, T. D.; Nava-Galindo, E.; Gong, P.; Haley, D.; Horton, R.; Katzarov, I.; Kermode J. R.; Liverani, C.; Stopher, M.; Sweeney, F. Understanding nad mitigating hydrogen embrittlement of steels: A review of experimental, modelling and design progress from atomistic to continuum. *J Mater Sci* **2018**, *53*, 6251-6290.

[5] Martin, L. M.; Connolly J.M.; Delrio, W. F.; Slifka, J. A. Hydrogen embrittlement in ferritic steels. *Appl. Phys. Rev*. **2020**, *7*, 041301.

[6] C. M. Ransom and P. J. Ficalora, Metall. Trans. A 11(5), 801 (1980).

[7] T. Wang, S. Wang, Q. Luo, Y.-W. Li, J. Wang, M. Beller, and J. Haijun, J. Phys. Chem. C 118(8), 4181 (2014).

[8] M. R. Shanabarger, Surf. Sci. 150(2), 451 (1985).

[9] M. Connolly, P. Bradley, A. Slifka, and E. Drexler, Rev. Sci. Instrum. 88(6), 063901 (2017).

[10] H. G. Nelson and J. E. Stein, "Gas-phase hydrogen permeation through alpha iron, 4130 steel, and 304 stainless steel from less than 100 C to near 600 C," Report No. NASA TN D-7265 (NASA, 1973).

[11] S. Dean, in Stress Corrosion—New Approaches (ASTM International, 1976).

[12] N. Yazdipour, A. J. Haq, K. Muzaka, and E. V. Pereloma, Comput. Mater. Sci.56, 49 (2012).

[13] A. Pundt and R. Kirchheim, Annu. Rev. Mater. Res. 36, 555 (2006).

[14] P. S. Lam, R. L. Sindelar, and T. M. Adams, Proceedings of the ASME Pressure Vessels and Piping Division Conference (ASME, 2008), p. 1.

[15] N. E. Nanninga, Y. S. Levy, E. S. Drexler, R. T. Condon, A. E. Stevenson, and A. J. Slifka, Corros. Sci. 59, 1 (2012).

[16] M. Wang, E. Akiyama, and K. Tsukaki, Mater. Sci. Eng., A 398, 37 (2005).

[17] 93. Y. Ogawa, H. Matsunaga, J. Yamabe, M. Yoshikawa, and S. Matsuoka, Int. J.
Fatigue 103, 223 (2017).

[18] C. San Marchi, D. G. Stalheim, B. P. Somerday, T. Boggess, K. A. Nibur, and S. Jansto, in Proceedings of the ASME Pressure Vessels and Piping Division/KPVP 2010 Conference (ASME, Bellevue, Washington, USA, 2010), p. 10.

[19] American Society of Mechanical Engineers, Standard: ASME B31.12-2019: Hydrogen Piping and Pipelines, 2019.

[20] S. Suresh and R. O. Ritchie, Met. Sci. 16(11), 529 (1982).

[21] A. J. Slifka, E. S. Drexler, R. L. Amaro, L. E. Hayden, D. G. Stalheim, D. S Lauria, and N. W. Hrabe, J. Pressure Vessel Technol. 140, 011407 (2018).

[22] R. L. Amaro, R. M. White, C. P. Looney, E. S. Drexler, and A. J. Slifka, J. Pressure Vessel Technol. 140(2), 021403 (2018).

[23] J. A. Ronevich, B. P. Somerday, and C. W. San Marchi, Int. J. Fatigue 82, 497 (2016).

[24] T. Neeraj, R. Srinivasan, and J. Li, Acta Mater. 60(13), 5160 (2012).

[25] M. L. Martin, M. Dadfarnia, A. Nagao, S. Wang, and P. Sofronis, Acta Mater. 165, 734 (2019).

[26] A. Nagao, M. Dadfarnia, B. P. Somerday, P. Sofronis, and R. O. Ritchie, J. Mech. Phys. Solids 112, 403 (2018).

[27] M. L. Martin, I. M. Robertson, and P. Sofronis, Acta Mater. 59(9), 3680 (2011).

[28] W. Krieger, S. V. Merzlikin, A. Bashir, A. Szczepaniak, H. Springer, and M. Rohwerder, Acta Mater. 144, 235 (2018).

[29] O. Sobol, G. Holzlechner, G. Nolze, T. Wirth, D. Eliezer, T. Boellinghaus, and W. E. S. Unger, Mater. Sci. Eng., A 676, 271 (2016).

[30] J. Takahashi, K. Kawakami, and Y. Kobayashi, Acta Mater. 153, 193 (2018).

[31] Y.-S. Chen, H. Lu, J. Liang, A. Rosenthal, H. Liu, G. Sneddon, I. McCarroll, Z. Zhao, W. Li, A. Guo, and J. M. Cairney, Science 367(6474), 171 (2020).